Magnetic excitations in NpBi

F. Bourdarot

CEA, Département de Recherche Fondamentale sur la Matière Condensée, SPSMS/MDN, 38054 Grenoble Cedex 9, France

J. Bossy

Institut Laue-Langevin, 156 X, 38042 Grenoble, France

P. Burlet and B. Fåk

CEA, Département de Recherche Fondamentale sur la Matière Condensée, SPSMS/MDN, 38054 Grenoble Cedex 9, France

P. Monachesi

Dipartimento di Fisica, Universita dell'Aquila, Via Vetoio, I-67010 l'Aquila, Italy

J. Rebizant

European Commission, JRC, European Institute for Transuranium Elements, Postfach 2340, 76125 Karlsruhe, Germany

L. P. Regnault

CEA, Département de Recherche Fondamentale sur la Matière Condensée, SPSMS/MDN, 38054 Grenoble Cedex 9, France

J. C. Spirlet

European Commission, JRC, European Institute for Transuranium Elements, Postfach 2340, 76125 Karlsruhe, Germany

O. Vogt

ETH, CH 8093 Zurich, Switzerland

(Received 19 May 1997)

We report inelastic neutron-scattering measurements on a single crystal of NpBi. The magnetic excitation spectrum consists of two branches with longitudinal and transverse polarization, respectively. The excitations are interpreted as spin waves in an antiferromagnetic triple-**k** type-*I* structure. With increasing temperature, the anisotropy gap decreases monotonously and disappears at T_N. As the ordered magnetic moment in NpBi has the free-ion Np^{3+} moment value, the anisotropy gap cannot originate from crystal-electric-field interactions, and the triple-**k** structure of NpBi is anticipated to be stabilized by two-ion quadrupolar terms. [S0163-1829(97)00746-7]

I. INTRODUCTION

The NaCl-type compounds of transition elements ($4f$ and $5f$) formed with anions of the V-A (monochalcogenides) and VI-A (monopnictides) columns of the periodic table show an extremely wide variety of magnetic behavior. Among them, the monopnictides of Ce and of the light actinides (U, Np, and Pu) present a special interest since the strong hybridization of the f electrons with the conduction electrons leads to unusual magnetic properties. In the last two decades, the availability of single crystals of these compounds has allowed numerous neutron-diffraction studies of their magnetic structures as well as of the phase diagrams they present under magnetic field, pressure, and anion dilution.[1,2] Inelastic neutron-scattering (INS) studies of the spin dynamics in these compounds are less numerous and almost exclusively limited to cerium and uranium compounds.[3] They are however of great interest, since the exchange and anisotropy parameters can be determined from the measured dispersion curves. In the special case of the multi-**k** magnetic ordering encountered frequently in these compounds, it has been experimentally observed[4,5] and explained[6] in USb (triple-**k** structure) that the spin-wave dis-

persion curves are different from that of a simple collinear ordering. Other compounds, in which triple-**k** structures have been determined by neutron diffraction, are the neptunium pnictides NpSb (Ref. 7), NpAs (at low temperature),[8] and NpBi.[9] In this paper, we will present INS measurements of the magnetic excitation spectrum carried out on a single crystal of NpBi.

NpBi orders antiferromagnetically below $T_N = 192.5$ K in a triple-**k** type-*I* structure, which results from the combination of the three Fourier components $\mathbf{m}_{k_x}$, $\mathbf{m}_{k_y}$, and $\mathbf{m}_{k_z}$ of wave vectors $\mathbf{k}_x$, $\mathbf{k}_y$, and $\mathbf{k}_z$, respectively ($\mathbf{k}_x = [100]$, $\mathbf{k}_y = [010]$, and $\mathbf{k}_z = [001]$). The magnetic moments point along the $\langle 111 \rangle$ directions and reach at low temperatures the value corresponding to the free Np^{3+} ion in an intermediate coupling scheme ($2.63\mu_B/\text{Np}$). Since NpBi has nearly the full moment, the predominant spin waves are transverse with the respect to the easy $\langle 111 \rangle$ axis, and the longitudinal spin excitations are negligible. It has been suggested that the multi-**k** antiferromagnetic structures could be the consequence of a competition between anisotropic exchange interactions and single-ion anisotropy[10] [essentially the crystal electric field (CEF)]. In this case, the anisotropic exchange interactions force the propagation vectors and the associated

Fourier components along the cubic axes. In the case of a collinear (single **k**) structure this leads to a stacking of ferromagnetic [001] planes. The interactions appear then strongly ferromagnetic in the plane and antiferromagnetic between the planes. The particular value of **k** depends on the details of these interplane interactions. The competing single-ion anisotropy can favor another easy direction than the fourfold axis. In this case, a multiaxial structure built from 2 ([110] easy axis) or 3 ([111] easy axis) **k** vectors is stabilized, minimizing simultaneously the exchange and the anisotropy energies. However, it is difficult to quantify the exchange interactions and the competing single-ion anisotropy because of hybridization effects. Theoretical models to interpret this behavior have been developed by Cooper and co-workers[11,12] in the framework of the Coqblin-Schrieffer Hamiltonian and by Takahashi and Kasuya[13] who consider a strong f-p hybridization.

The aim of this study was to confirm the triple-**k** structure and to compare the magnetic excitation spectrum of NpBi to the model used for USb. Section II describes the experimental details. The results are analyzed in Sec. III and the discussion in Sec. IV concludes the paper.

II. EXPERIMENTAL DETAILS

We have performed INS measurements on a single crystal grown at the European Institute for Transuranium Elements by the mineralization technique. It has the shape of a parallelepiped of $13 \times 6.7 \times 2.6$ mm^3 and has been oriented and encapsulated in a cylindrical double-wall aluminum container. The faces of the parallelepiped are perpendicular to the four-fold axes. The measurements were performed on the three-axes spectrometer IN8 installed on a thermal beam of the high-flux reactor at the Institut Laue Langevin. To investigate the energy range $8 < E < 20$ meV, a vertically focusing copper monochromator [Cu(111)] and a pyrolitic graphite [PG(002)] analyzer focused in the vertical and horizontal planes were used. The collimation was fully relaxed, which gave an energy resolution (for incoherent elastic scattering) of about 3.5 meV for a fixed final energy of 34.8 meV. A pyrolitic graphite filter placed in front of the analyzer was used to reduce the $\lambda/2$ contribution. All presented neutron data have been normalized to the same monitor value $M = 10\,000$ corrected for higher-order contamination. Complementary measurements were performed for a fixed final energy of 14.7 meV, using a PG(002) vertically focused monochromator and $40'$ collimators after the monochromator, between the sample and the analyzer, and after the analyzer. The energy resolution improved to 1 meV at the expense of an eightfold reduction in intensity. The crystal was mounted in a helium-flow cryostat with the $[1,-1,0]$ axis vertical so that the main symmetry directions [001], [110], and [111] were all in the horizontal scattering plane.

III. RESULTS

Energy scans performed at low temperatures ($T = 10$ K) and above T_N ($T = 210$ K) at the magnetic zone center **Q** $= (110)$, which corresponds to the propagation vector $\mathbf{k}_z = (001)$, are shown in Fig. 1. In such scans, fluctuations parallel and perpendicular to $\mathbf{k}_z$ are simultaneously probed.
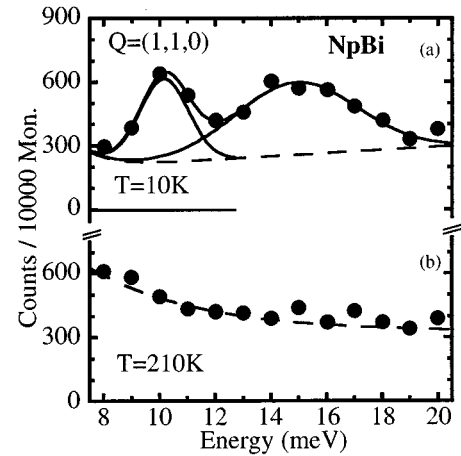

FIG. 1. Energy scans at **Q** $= (1,1,0)$ for (a) $T = 10$ K and (b) $T = 210$ K. A Gaussian function is used to fit the excitations. The dashed lines show the estimated background level.

At low temperatures ($T = 10$ K), two inelastic peaks are observed, respectively, at 10 and 15 meV. Instrumental resolution effects make the width of the high-energy peak approximately two times larger than that of the low-energy peak. Qualitatively, this is connected to the relative orientation between the resolution ellipsoid and the slope of the dispersion curve. Above T_N, only a monotonous background is seen and the absence of any peaks demonstrate the magnetic origin of the excitations observed at low temperatures. The extra intensity observed below 12 meV could correspond to an increase of the acoustic phonon intensity and of multiphonon scattering. Figure 2 compares two low-temperature energy scans performed at the scattering vector **Q** $= (1,1,0.1)$, for which both transverse and longitudinal excitations are probed, and the scattering vector **Q** $= (0,0,1.1)$, for which only transverse excitations contribute. The absence of the low-energy excitation at **Q** $= (0,0,1.1)$ proves its longitudinal character [measurements have not been performed at **Q** $= (001)$ because of a large background coming from the direct beam]. The low-energy longitudinal excitation corresponds to the component of the transverse moment fluctuations along the z axis parallel to the propagation vector $\mathbf{k}_z$
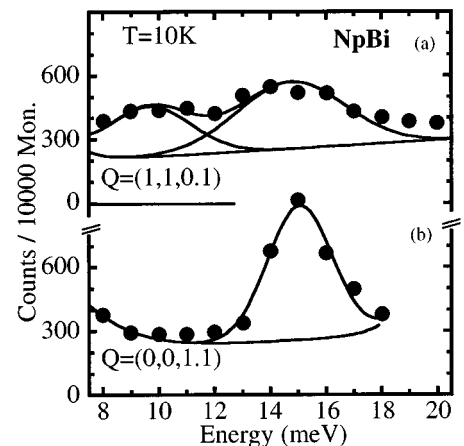

FIG. 2. Energy scans at $T = 10$ K for (a) **Q** $= (1,1,0.1)$ and (b) **Q** $= (0,0,1.1)$.
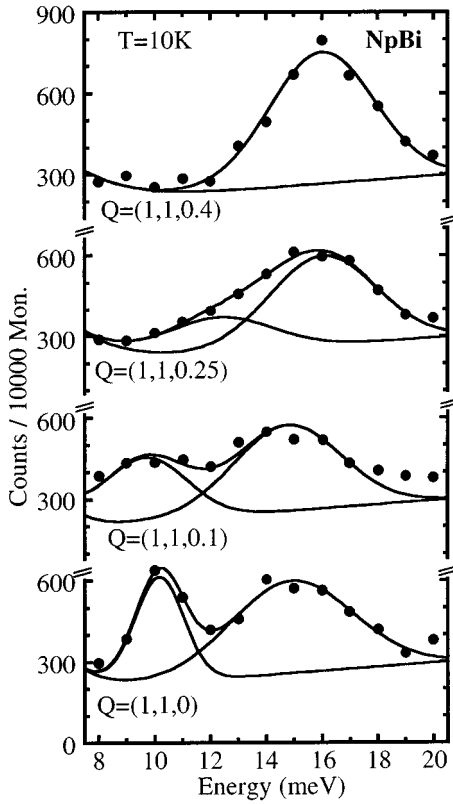
FIG. 3. Energy scans at $T=10$ K for $\mathbf{Q}=(1,1,\zeta)$ ($\zeta=0$, 0.1, 0.25, 0.4). The background is the same for all the scans. A Gaussian function is used to fit the excitations.
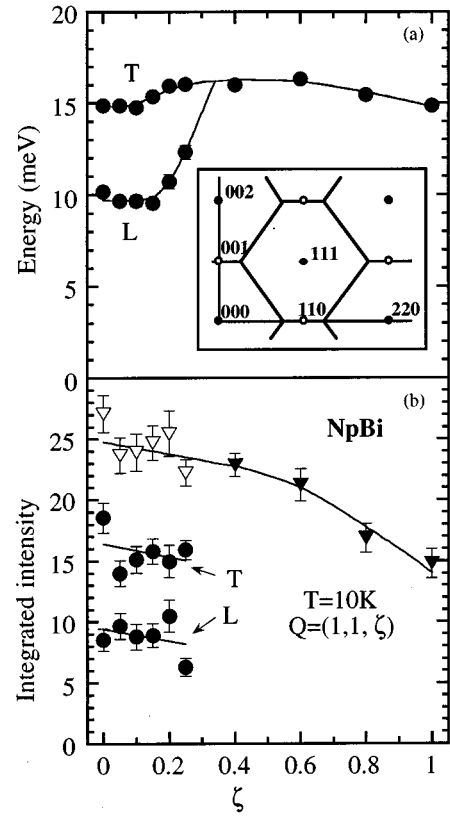

FIG. 4. (a) Dispersion along $\mathbf{Q}=(1,1,\zeta)$ at $T=10$ K and (b) integrated intensity. L denotes the longitudinal and T the transverse mode. The symbol ($\triangledown$) corresponds to the sum of the individual intensities of the two peaks and the full symbols ($\blacktriangledown$ and $\bullet$) correspond to the intensities of the observed peaks. The inset shows the Brillouin zone in the scattering plane.

(recall that the moments are along the $\langle 111 \rangle$ directions while the Fourier components are parallel to their respective $\mathbf{k}$ vectors). On the other hand, the transverse excitation at higher energies corresponds to components of the transverse moment fluctuations perpendicular to $\mathbf{k}_z$. Figure 3 shows typical energy scans performed at scattering vectors $\mathbf{Q}=(11\zeta)$ for $\zeta=0$, 0.1, 0.2, and, 0.4 rlu (reciporocal-lattice units). From these scans and similar scans performed along the $[\zeta\zeta 0]$ direction, we have been able to extract the dispersion curves shown, respectively, in Figs. 4(a) and 5(a). In both directions, two distinct branches are observed in the range of ζ between 0 and approximately 0.3. These excitations were fitted using two Gaussians on a sloping background. The upper mode displays only a weak dispersion, while the energy of the lower mode increases from 10 meV for $\zeta=0$ to 15 meV for $\zeta\approx 0.3$. Above $\zeta\approx 0.3$, only one peak is observed. This could mean that the transverse and longitudinal excitations have the same energy, or that the longitudinal mode is no longer observable because the amplitude vanishes.

An indication that the two excitations may exist in the whole ζ range but with identical energies for $\zeta>0.3$ is given by the analysis of the ζ dependence of the integrated intensities given in Figs. 4(b) and 5(b). Within the accuracy of the measurements, the intensity of the unique peak above $\zeta=0.3$ is equivalent to the sum of the individual intensities of the two peaks measured for $\zeta<0.3$. However, it could also be that the low-energy excitation disappear for $\zeta>0.3$, as suggested by its decreasing amplitude with ζ (see Fig. 3).

In the $[00\zeta]$ direction, the dispersion is initially very

weak. Although it is not evident from Fig. 4(a) that the dispersion curve for the longitudinal mode has its minimum at $\zeta=0$, this can be inferred from the decrease of the peak height and increase of the width of the low-energy peak as ζ increases, as seen in Fig. 3. The difference in the spin-wave dispersion between the $[\zeta\zeta 0]$ direction and the $[00\zeta]$ direction corresponds certainly to anisotropy effects, resulting from exchange, single-ion, or two-ion terms.

Figure 6 shows energy scans at $\mathbf{Q}=(110)$ performed at temperatures $T=10$, 60, 111, and 159 K. As the temperature increases, the energy of the longitudinal excitation decreases from 10.2 meV at $T=10$ K down to 7.3 meV at $T=111$ K, whereas the transverse excitation decreases from 14.9 meV at low temperatures down to 8.9 meV at $T=159$ K. The inset in Fig. 6 shows the corresponding temperature dependencies of the T and L modes. At higher temperatures, the magnetic excitations are no longer detectable above the increasing low-energy nuclear intensity. However, as shown in the inset of Fig. 6, the observed temperature dependence of the excitation energies is consistent with a monotonous behavior and vanishing gaps at T_N. Measurements with improved resolution, performed in order to follow the gap at higher temperatures, were without success due to the important loss in intensity.

A few measurements of the phonon dispersions were performed with both high and low resolution, in order to inves-
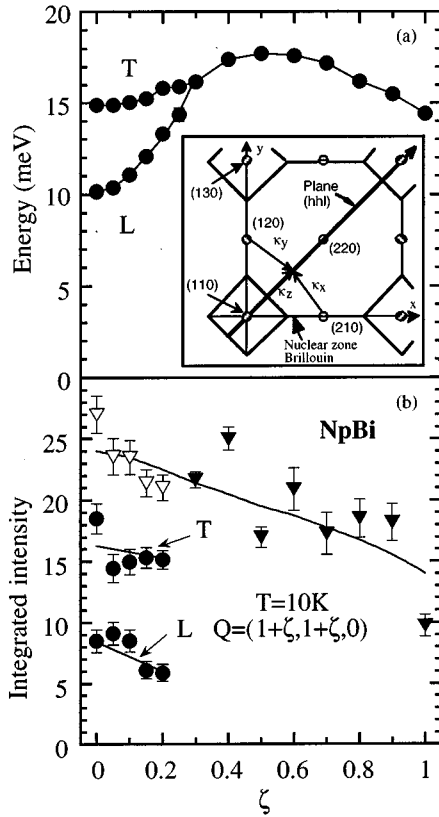
FIG. 5. (a) Dispersion along $\mathbf{Q}=(1+\zeta,1+\zeta,0)$ at $T=10$ K and (b) integrated intensity. Symbols as in Fig. 4. The inset shows the three κ vectors corresponding to $\mathbf{Q}=(1+\zeta,1+\zeta,0)$ (two of the modes are degenerate in the [110] direction, since κ_x and κ_y are symmetric).

tigate possible magnetoelastic coupling. In general, the phonons in NpBi are softer compared to USb, as expected from the difference in atomic masses.

IV. DISCUSSION

A first result of this study is the confirmation of the triple-**k** nature of the type-*I* antiferromagnetic ordering of NpBi previously deduced from neutron-diffraction measurements.[9] Indeed, the magnetic excitation spectrum consists of two branches with longitudinal and transverse polarization, respectively. As shown by Jensen and Bak,[6] the presence of a low-energy branch with a longitudinal polarization is a signature of triple-**k** ordering. Such a mode does not exist in a collinear structure (in which all the excitations are transverse), even taking into account the 3 K domains. This statement is discussed in the Appendix.

The trivalent nature of the neptunium ion (Np^{3+}, $J=4$) is determined from the Mössbauer isomer shift. In cubic symmetry, the $^5I_4$ multiplet is split by the CEF into four states: a singlet Γ_1, a nonmagnetic doublet Γ_3, and two triplets, Γ_4 and Γ_5, with magnetic moments of $0.31\mu_B$ and $1.54\mu_B$, respectively (Table I). These moments are much smaller than the ordered moment of $2.63\mu_B$ measured by neutron diffraction and Mössbauer spectroscopy. Table I
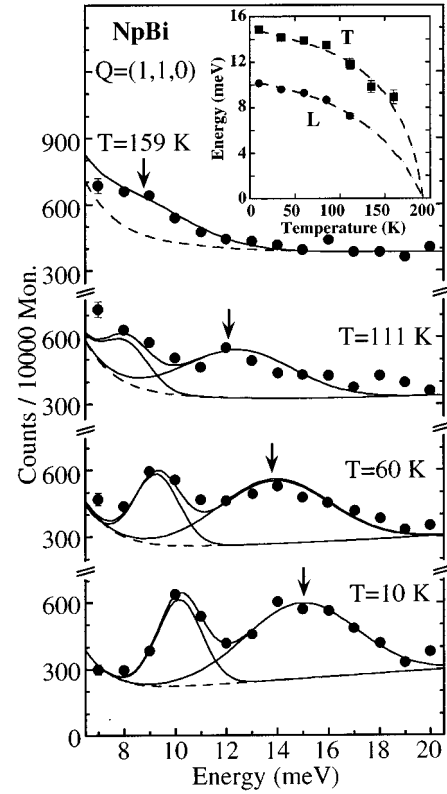

FIG. 6. Energy scans at $\mathbf{Q}=(1,1,0)$ at different temperatures. The background shown by the dashed line increases as the Bose factor. The arrow indicates the energy of the transverse mode. The inset shows the temperature dependence of the longitudinal and the transverse modes.

shows a comparison between the Mössbauer characteristics (ordered moment, isomer shift, and quadrupolar interaction) of different magnetic states with the experimental results for NpBi. The values correspond to pure CEF states without
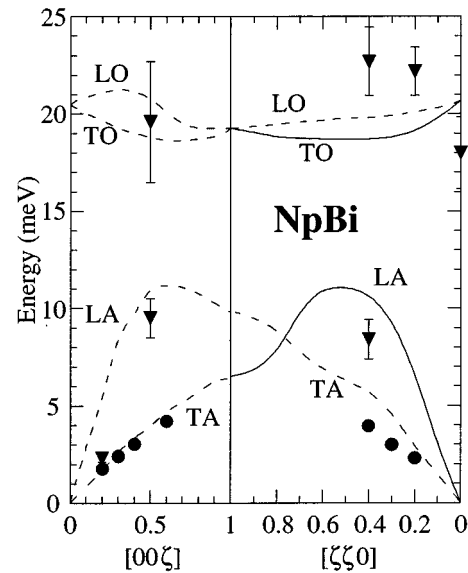

FIG. 7. Phonon dispersion curves of NpBi. The dashed lines represent the USb phonon dispersion (cf. Ref. 3). The symbols ▼ and ● correspond to the longitudinal and transverse phonons of NpBi, respectively.

TABLE I. Ordered moment m_0, the isomer shift δ_{is}, and quadrupolar interaction e^2qQ of Np^{3+} free ion ($5f^4$ configuration) compared with two different CEF states and with observed values of NpBi.

	m_0 (μ_B)	$\delta_{is}/NpA1_2$ (mm/s)	e^2qQ
Np^{3+} free ion	2.57[a]	38	-27.3
Γ_5	1.54[a]	38	-3.9
Γ_4	0.31[a]	38	13.7
NpBi	2.63 (11)	25.1 (3)	-31.1

[a]For intermediate coupling.

exchange interactions. The moment in the CEF ground state can be increased in the presence of exchange interactions. Such a model including both crystal electric field and anisotropic exchange interaction was previously developed for USb.[5] For NpBi, this model, when used with parameters giving the correct Néel temperature and anisotropy gap at $\mathbf{q} = (001)$, does not give an accurate description of the dispersion curve, and the moment obtained is only about $2.1\mu_B$ for the Γ_5 state, with the moment along the $\langle 100 \rangle$ axis. An easy $\langle 111 \rangle$ axis can be obtained, associated with a moment in the ground state (Γ_5) of only $1.7\mu_B$. These values are well outside of the experimental errors of the measured ordered moment. We conclude that the experimental moment $[2.63(4)\mu_B]$ corresponds to that of the Np^{3+} free ion in the intermediate coupling scheme ($2.59\mu_B$). The ground state $J = J_z$ is corroborated by the results of Mössbauer spectroscopy, which show that the quadrupolar interaction in NpBi corresponds to the free ion Np^{3+}, and not to the quadrupolar interactions expected for the CEF ground states Γ_4 or Γ_5 (cf. Table I). Furthermore, the high-temperature magnetic susceptibility corresponds to an effective moment of $2.90(5)\mu_B$, which is in perfect agreement with the result of a free-ion Np^{3+} state ($m_{eff} = 2.87\mu_B$). It is clear from these observations that the gap which has been obtained in the magnetic dispersion curves cannot be explained from any CEF splitting. To our opinion, the gap of 10 meV that has been observed at $\mathbf{q} = (001)$ originates from other interactions, which could be anisotropic as suggested by the different dispersion curves along the $[00\zeta]$ and $[\zeta\zeta 0]$ directions.

NpBi presents strong similarities with the isostructural U-based compound USb. Both compounds order in the

TABLE II. Ordered moment m_0 for the $5f^3$ configuration of U^{3+}. Free ion as well as cubic crystal-field Γ state values are given in intermediate coupling scheme. These values are compared with the moment of USb.

	m_0 (μ_B)
U^{3+} free ion	3.68[a]
Γ_6	1.38[a]
Γ_8^1	1.07–2.43[a]
Γ_8^2	1.54–2.3[a]
Γ_8^1 with exchange interactions (Ref. 6)	2.73 ± 0.05
USb	2.8 (1)

[a]For an intermediate coupling.

triple-$\mathbf{k}$ type-I structure below a relatively high Néel temperature of 192 and 213 K, respectively. Well defined spin waves with an anisotropy gap are observed at low temperatures. The spin-wave damping increases with temperature. In spite of these similarities, some important differences must be pointed out. The behavior of USb can be described with a CEF scheme with Γ_8^1 triplet as ground state and additional anisotropic exchange interactions (see Table II). Such a model is in good agreement with the spin-wave dispersion curves, the Néel temperature, the value of the ordered moment, and the moment direction. It was claimed in Ref. 14 that the spin-wave dispersion of USb is isotropic along the [100], [110], and [111] directions, which implies that the quadrupolar interactions are much weaker than the CEF. The situation is completely different in NpBi, where the observed ordered magnetic moment in NpBi is only compatible with a fully degenerate $J = 4$ multiplet ground state, and corresponds therefore to a small CEF splitting. The slightly anisotropic dispersion observed along the [100] and [110] directions may originate in this case from quadrupolar interactions, given by the Hamiltonian

$$Q = - \sum_{i,j} K_{i,j}(k) Q_i Q_j,$$

where $K_{i,j}(k)$ are the Fourier components of the quadrupolar interaction and $\mathbf{Q_k}$ are the Fourier transform of the quadrupolar components, $Q = \langle O_2^0 \rangle$, $\langle O_2^2 \rangle$, and $\langle P_{ij} \rangle$ (c.f. Ref. 15 for the notation). In NpBi, the local magnetic symmetry of the neptunium site is trigonal, and the dominant quadrupolar term is $\langle P_{ij} \rangle$. An analysis of the stability of antiferromagnetically ordered multi-$\mathbf{k}$ structures in simple cubic compounds has shown that this structure can be stabilized by an antiferroquadrupolar interaction.[15] A full analysis of the magnetic behavior of NpBi along these lines would require a more complete set of experimental data.

The INS measurements in USb have shown that the transverse acoustic phonon has exactly the same energy as the magnetic excitation at the X point $[\mathbf{Q} = (110)]$.[14] However, it was concluded that this is accidental and that there is no strong magnetoelastic coupling in USb. In NpBi, near the X point $[\mathbf{Q} = (1,1,0)$ and $\mathbf{Q} = (0,0,1.1)]$, no phonon was observed in the range of energy (8–20 meV) where spin waves are detected. This excludes a strong magnetoelastic term in the Hamiltonian in NpBi as well.

From the present study, we can conclude that the antiferromagnetic triple-$\mathbf{k}$ type-I structure is stabilized in NpBi by dominant two-ion interaction terms: the anisotropic exchange and the quadrupolar interaction, with only a weak CEF and no magnetoelastic coupling. This is in contrast to USb, where the anisotropic exchange term and the CEF terms are dominating. However, it is not clear in the case of USb that the $\langle P_{ij} \rangle$ quadrupolar terms are negligible, as Hälg and Furrer[5] assumed. The differences between NpBi and USb clearly illustrate that the magnetic properties of actinide compounds are very sensitive to small changes in the different interactions.

zyk of EITU, Karlsruhe for their expertise in crystal growth and encapsulation. The Transuranium and Radioprotection group at the ILL is acknowledged for arranging the safety procedures and assistance for this experiment. The high purity Np metal used for the fabrication of the sample was made available through a loan agreement between the Lawrence Livermore National Laboratory and EITU in the framework of a collaboration involving the Lawrence Livermore and Los Alamos National Laboratories, and the U.S. Department of Energy.

APPENDIX: DYNAMIC COMPONENTS IN AN fcc ANTIFERROMAGNETIC TRIPLE-k TYPE-*I* STRUCTURE

In an ordered state the magnetic moment at the site r and time t can be written in a classical picture as the sum of a static ($\mathbf{m}_{\mathrm{sta}}$) and a dynamic ($\mathbf{m}_{\mathrm{dyn}}$) component:

$$\mathbf{m}(r,t) = \mathbf{m}_{\mathrm{sta}}(r) + \mathbf{m}_{\mathrm{dyn}}(r,t).$$

On each site, we consider a local coordinate system $(\mathbf{u}_i, \mathbf{v}_i, \mathbf{w}_i)$, with $\mathbf{w}_i$ along the direction of the static component. The dynamic part (transverse component) precesses around the static component and it can be described using the two vectors $(\mathbf{u}_i, \mathbf{v}_i)$ as

$$\mathbf{m}_{\mathrm{dyn}}(\mathbf{r}_i, t) = \mathbf{m}_{\mathrm{dyn}}(e_i^{i(\phi-\omega t)}[(\mathbf{u}_i - i\mathbf{v}_i)/2]$$
$$+ e_i^{-i(\phi-\omega t)}[(\mathbf{u}_i + i\mathbf{v}_i)/2)]. \quad (A1)$$

Spin waves are collective modes, for which there is a relation between the phases ϕ_i of the different sites. In a physical picture of spin waves, the phase ϕ_i can be written as

$$\phi_i = 2\pi\kappa \cdot \mathbf{r}_i,$$

where κ is the reduced wave vector defined with respect to the antiferromagnetic zone center (see inset Fig. 5) by

$$\mathbf{Q} = \tau + \mathbf{q} = \tau + \mathbf{k} + \kappa, \quad (A2)$$

where $\mathbf{Q}$ is the scattering vector, $\mathbf{k}$ the propagation vector, and τ a reciprocal lattice vector.

For a triple-$\mathbf{k}$ structure the static part of the moment at a site $\mathbf{r}_i = (x_i, y_i, z_i)$ lies along the direction $[(-1)^{x_i}, (-1)^{y_i}, (-1)^{z_i}]$, which allows to define basal unitary vectors of the local system as

$$\mathbf{w}_i = \frac{1}{\sqrt{3}}[(-1)^{x_i}, (-1)^{y_i}, (-1)^{z_i}],$$

$$\mathbf{v}_i = \frac{1}{\sqrt{2}}[(-1)^{x_i}, -(-1)^{y_i}, 0],$$

$$\mathbf{u}_i = \frac{1}{\sqrt{6}}[-(-1)^{x_i}, -(-1)^{y_i}, 2(-1)^{z_i}].$$

According to relation (A1), the dynamic part has components along the three cubic axes

$$\mathbf{m}_{\mathrm{dyn}}(r,t) = \Delta \mathbf{m}_{x_i} + \Delta \mathbf{m}_{y_i} + \Delta \mathbf{m}_{z_i},$$

with

$$\Delta m_{x_i} = -\Delta m[e^{i(2\pi\kappa \cdot \mathbf{r_i} - \omega t)}d + e^{-i(2\pi\kappa \cdot \mathbf{r_i} - \omega t)}d^*]e^{i(2\pi\mathbf{k_x} \cdot \mathbf{r_i})},$$

$$\Delta m_{y_i} = -\Delta m[e^{i(2\pi\kappa \cdot \mathbf{r_i} - \omega t)}d^* + e^{-i(2\pi\kappa \cdot \mathbf{r_i} - \omega t)}d]e^{i(2\pi\mathbf{k_y} \cdot \mathbf{r_i})},$$

$$\Delta m_{z_i} = \Delta mf[e^{i(2\pi\kappa \cdot \mathbf{r_i} - \omega t)} + e^{-i(2\pi\kappa \cdot \mathbf{r_i} - \omega t)}]e^{i(2\pi\mathbf{k_z} \cdot \mathbf{r_i})},$$
$$(A3)$$

$\mathbf{d} = (1/\sqrt{6} + \mathbf{i}/\sqrt{2})/2$, $\mathbf{f} = 1/\sqrt{6}$ and d^* is the complex conjugate of d.

For any reduced wave vector $\mathbf{q}$, three κ_i vectors are derived from Eq. (A2), by considering the three $\mathbf{k}_i$ vectors. Thus, in the general case, three excitations must be observed at any scattering vector $\mathbf{Q}$. These excitations may be partly degenerate in certain high symmetry directions. Since there are four magnetic atoms in the magnetic cell, there is also a structure factor associated with each mode,

$$\mathbf{F}_{\mathrm{Me}} = \sum_{\substack{\mathbf{r_i}\ \mathrm{in} \\ \mathrm{magn.\ cell}}} \Delta m_{j_i} \mathbf{e}^{i(2\pi Q \cdot \mathbf{r_i})}$$

where $j = x$, y, and z and Δm_{j_i} is given by the formula (A3). At the magnetic zone center [e.g., $\mathbf{Q} = (001)$ or $\mathbf{Q} = (110)$], there are two excitation energies: the low-energy excitation (E_1) if $\kappa = (000)$ and the high energy excitation (E_2) if $\kappa = (100)$, (010), or (001). In the case of a single-k structure, the scans performed at $\mathbf{Q} = (001)$ and $\mathbf{Q} = (110)$ show two peaks if the three domains ($\mathbf{k}_x$, $\mathbf{k}_y$, and $\mathbf{k}_z$) exist. Of course, if there is only one domain, only one peak appears in the scans. In the case of a triple-k structure, the scan performed at $\mathbf{Q} = (110)$ shows two peaks, while the scan performed at $\mathbf{Q} = (001)$ has only one peak at high energy. The low-energy peak corresponds to magnetic fluctuations along the magnetic wave vector (so defined as longitudinal character) but the actual moment fluctuations are purely transverse with respect to the local moment direction. The absence of this excitation at $\mathbf{Q} = (001)$, which follows from that $\mathbf{Q}$ is prependicular to $\Delta\mathbf{m}$, is the signature of the triple-k structure. The longitudinal and transverse modes at the Γ point have been well represented in Ref. 16. Along the symmetry directions [ξ00], [$\xi\xi$0] and [$\xi\xi\xi$], the number of observed branches is limited due to energy degeneracy.

[1] J. Rossat-Mignod, G. H. Lander, and P. Burlet, in *Handbook of Physics and Chemistry of the Actinides*, edited by A. J. Freeman and G. H. Lander (North-Holland, Amsterdam, 1984), Vol. 1, p. 415.

[2] O. Vogt and K. Mattenberger, in *Handbook on the Physics and Chemistry of the Rare Earths*, edited by K. Gschneidner, L. Eyring, G. H. Lander, and G. Choppin (Elsevier, Amsterdam, 1993), Vol. 17, Chap. 114, p. 301.

[3] E. Holland-Moritz and G. H. Lander, in *Handbook on the Physics and Chemistry of Rare Earths*, edited by A. J. Freeman and G. H. Lander (North-Holland, Amsterdam, 1994), Vol. 19, Chap. 130, p. 1.

[4] G. H. Lander and W. G. Stirling, Phys. Rev. B **21**, 436 (1980).

[5] B. Hälg and A. Furrer, Phys. Rev. B **34**, 6258 (1986).

[6] J. Jensen and P. Bak, Phys. Rev. B **23**, 6180 (1981).

[7] J. P. Sanchez, P. Burlet, S. Quezel, D. Bonnisseau, J. Rossat-Mignod, J. C. Spirlet, J. Rebizant, and O. Vogt, Solid State Commun. **67**, 999 (1988).

[8] P. Burlet, D. Bonisseau, S. Quezel, J. Rossat-Mignod, J. C. Spirlet, and O. Vogt, J. Magn. Magn. Mater. **63-64**, 151 (1987).

[9] P. Burlet, F. Bourdarot, J. Rossat-Mignod, J. P. Sanchez, J. C. Spirlet, J. Rebizant, and O. Vogt, Physica B **180-181**, 131 (1992).

[10] J. Rossat-Mignod, in *Neutron Scattering in Condensed Matter Research*, edited by K. Sköld and D. L. Price (Academic, New York, 1986), Chap. 19.

[11] R. Siemann and B. R. Cooper, Phys. Rev. Lett. **44**, 1015 (1980).

[12] N. Kioussis and B. R. Cooper, Phys. Rev. B **34**, 3261 (1986).

[13] H. Takahaski and T. Kasuya, J. Phys. C **18**, 2697 (1985).

[14] M. Hagen, W. G. Stirling, and G. H. Lander, Phys. Rev. B **37**, 1846 (1988).

[15] M. Amara and P. Morin, Physica B **205**, 379 (1995).

[16] D. Delacôte, Ph.D. thesis, University of Grenoble, 1981.